On the Capacity of Generalized-K Fading MIMO Channels

Michail Matthaiou, Nestor D. Chatzidiamantis, George K. Karagiannidis, and Josef A. Nossek, *Fellow, IEEE*

***Abstract*—This correspondence explores the ergodic capacity of multiple-input multiple-output (MIMO) systems operating in generalized-K fading conditions. Using some recent results on majorization theory, we derive an analytical capacity bound which is applicable for arbitrary values of the signal-to-noise ratio (SNR) and number of antenna elements. In addition, we deduce simple bound approximations in the high-SNR regime and demonstrate that the effects of small and large-scale fading are decoupled. A similar statistical analysis is carried out for MIMO channels under K-fading, which represents a special case of generalized-K fading that can be tackled via the Wishart matrix theory. The implications of the model parameters on the bound performance are also investigated via Monte Carlo simulations.**

***Index Terms*—Ergodic capacity, generalized-K fading, majorization theory, MIMO systems.**

I. Introduction

Over the past decade, numerous publications have been reported on the statistical and capacity characterization of MIMO systems. The majority of them, however, adopts the common assumption of Rayleigh [1]–[3] or Ricean [4], [5] fading conditions. In these cases, the channel statistics are jointly Gaussian and the mathematical formulations can be carried out using elements of the well-known Wishart matrix theory, which simplifies extensively the overall analysis. Some theoretical investigations and measurement campaigns [6], [7], however, have demonstrated that the Nakagami-m distribution [8] yields a better fit with real-time data for various measured channels and, more importantly, encompasses both Rayleigh/Ricean distributions as special cases. This reveals that deriving performance bounds for MIMO Nakagami-m channels is a highly interesting topic. Surprisingly, little is still known for these MIMO channels due to the difficulty in manipulating the non-Gaussian joint channel statistics, and especially the joint eigenvalue distribution, when the channel experiences Nakagami fading. Only recently, the authors in [9] considered the eigenvalue statistics of 2×2, 2×3 configurations and provided large system capacity expressions.

Nevertheless, a seminal work in this area was presented in [10], where the authors used tools from majorization theory to derive tight upper and lower bounds for Nakagami-m/lognormal MIMO channels. Their final formulas, however, were given in integral form [10, Theorems 4–5] and the proposed bounds were numerically approximated via Gauss–Hermite polynomials, although such a technique comes in contrast with the definition of the bound. Furthermore, the authors acknowledge this approximation as time consuming, especially at low SNRs, and not amenable to further manipulations.

Thus, capitalizing on the technique of [10], we herein deduce novel analytical bounds for the ergodic capacity of MIMO systems experiencing generalized-K fading. This is a generic model that occurs when small-scale fading is modeled via the Nakagami-m distribution and large-scale fading via the gamma distribution. This model has been demonstrated to effectively approximate most of the fading and shadowing effects occurring in wireless channels, and also to be analytically friendlier than the Nakagami-m/lognormal model [11]–[14].

In this correspondence, we first provide a general analytical upper bound for the ergodic capacity of generalized-K MIMO channels for arbitrary SNR. In contrast to [10], the proposed bound is expressed in terms of Meijer's G-function which can be easily evaluated and efficiently programmed in most standard software packages (e.g., Maple, Mathematica). For the case of non-integer arguments of the Meijer's G-function, an alternative closed-form bound expression is provided as a finite weighted sum of hypergeometric/digamma functions. The asymptotic bound performance in the high-SNR regime is assessed and a tractable expression is deduced which indicates that the effects of small and large-scale fading are decoupled.

We further elaborate on the special case of K (composite Rayleigh/gamma fading) MIMO channels [15], [16], by introducing two insightful affine capacity expansions. We also present closed-form high-SNR approximations for the ergodic capacity and the variance of the mutual information (MI) followed by a tight lower capacity bound.

II. MIMO System Model

We consider a typical distributed MIMO (D-MIMO) system with N_r receive antennas and L radio ports each connected to N_t transmit antennas and also define $s \triangleq \min(LN_t, N_r)$, $t \triangleq \max(LN_t, N_r)$. Then, the input-output relationship reads

$$\mathbf{y} = \sqrt{\gamma}\mathbf{H}\mathbf{\Xi}^{1/2}\mathbf{x} + \mathbf{n} \tag{1}$$

where $\mathbf{x} \in \mathbb{C}^{LN_t\times 1}$ and $\mathbf{y} \in \mathbb{C}^{N_r\times 1}$ are the transmitted and received signal vectors while $\mathbf{n} \sim \mathcal{CN}(\mathbf{0}, \mathbf{I}_{N_r})$ is the complex AWGN and γ corresponds to the average SNR. The entries of the diagonal matrix $\mathbf{\Xi} \in \mathbb{R}^{LN_t\times LN_t}$ represent the large-scale effects, and hence $\mathbf{\Xi} = \operatorname{diag}\{\mathbf{I}_{N_t}\xi_i/D_i^v\}_{i=1}^{L}$ where $D_i, i = 1,\ldots,L$ denotes the distance between the receiver and the ith radio port while v is the path-loss exponent with typical values ranging from 2–6. The large-scale fading coefficients $\xi_i, i = 1,\ldots,L$, are modeled as i.i.d. gamma random variables (RVs), $\xi_i \sim \operatorname{Gamma}(k_i, \Omega_i)$, or

$$p(\xi_i) = \frac{\xi_i^{k_i-1}}{\Gamma(k_i)\Omega_i^{k_i}}\exp\left(-\frac{\xi_i}{\Omega_i}\right), \quad \xi_i, \Omega_i, k_i \geq 0 \tag{2}$$

where k_i, $\Omega_i = \mathcal{E}[\xi_i]/k_i$, are the shape and scale parameters of the gamma distribution respectively while $\Gamma(\cdot)$ is the gamma function and $\mathcal{E}[\cdot]$ is the expectation of a RV. The entries of the channel matrix $\mathbf{H} \in \mathbb{C}^{N_r\times LN_t}$ are assumed to be i.i.d. RVs with uniformly distributed phase in $[0,\ 2\pi)$, while their amplitude $x = |h_{i,j}|$ follows a Nakagami-m distribution

$$p(x) = \frac{2}{\Gamma(m)}\left(\frac{m}{\Omega}\right)^m x^{2m-1}e^{-(m/\Omega)x^2}, \quad x \geq 0,\ m \geq \frac{1}{2} \tag{3}$$

where $\Omega = \mathcal{E}[x^2]$ is the average power, which will be assumed to be equal to unity [15], [16]. Then, the squared Nakagami-m envelope, $r = x^2$, is distributed as $r \sim \operatorname{Gamma}(m, 1/m)$.

Manuscript received June 21, 2010; accepted July 02, 2010. Date of publication July 15, 2010; date of current version October 13, 2010. The associate editor coordinating the review of this manuscript and approving it for publication was Dr. Walid Hachem.

M. Matthaiou was with the Institute for Circuit Theory and Signal Processing, TU München, Germany. He is now with the Department of Signals and Systems, Chalmers University of Technology, SE-412 96, Gothenburg, Sweden (e-mail: michail.matthaiou@chalmers.se).

N. D. Chatzidiamantis and G. K. Karagiannidis are with the Department of Electrical and Computer Engineering, Aristotle University of Thessaloniki, 54 124, Thessaloniki, Greece (email: nestoras@auth.gr; geokarag@auth.gr).

J. A. Nossek is with the Institute for Circuit Theory and Signal Processing, Technische Universität München (TUM), 80333, Munich, Germany (e-mail: nossek@nws.ei.tum.de).

Digital Object Identifier 10.1109/TSP.2010.2058108

III. Ergodic Capacity Upper Bound

We assume that the receiver has perfect channel state information (CSI) while the transmitter has nor statistical neither instantaneous CSI and as such performs uniform power allocation across all data streams. Then, the MIMO MI reads as

$$\mathcal{I} = \log_2\left(\det\left(\mathbf{I}_{N_r} + \frac{\gamma}{LN_t}\mathbf{H}\Xi\mathbf{H}^\dagger\right)\right) \text{ (bits/s/Hz)} \quad (4)$$

where $(\cdot)^\dagger$ denotes Hermitian transpose, while the MIMO ergodic capacity is given by

$$C_{\text{erg}} = \mathcal{E}\left[\mathcal{I}\right] = \mathcal{E}\left[\log_2\left(\det\left(\mathbf{I}_{LN_t} + \frac{\gamma}{LN_t}\mathbf{Z}^\dagger\mathbf{Z}\right)\right)\right] \quad (5)$$

where $\mathbf{Z} = \mathbf{H}\Xi^{1/2}$ and the expectation is taken over all realizations of $\mathbf{H}$ and Ξ (or likewise $\mathbf{Z}$). Using similar arguments as in [10, eq. (36)-(37)], we can directly introduce the following upper bound C_{up} for the MIMO ergodic capacity[1]:

$$C_{\text{erg}} \leq C_{\text{up}} = \mathcal{E}\left[\sum_{i=1}^{s}\log_2\left(1 + \frac{\gamma}{LN_t}z_{ii}\right)\right] \quad (6)$$

where $z_{ii} \in \mathbb{R}^+, i = 1, \ldots, s$ are the real, non-negative diagonal elements of $\mathbf{Z}^\dagger\mathbf{Z}$. We now recall that the sum of n i.i.d. gamma RVs with common scale parameter θ and shape parameters $\{k_i\}_{i=1}^n$ is also gamma distributed with parameters $(\sum_{i=1}^n k_i, \theta)$. Then, we can see that the diagonal elements z_{ii} are essentially weighted sums of i.i.d. gamma RVs with each weight factor being a gamma RV as well.

Theorem 1: The ergodic capacity (5) is upper bounded by

$$C_{\text{up}} = \frac{N_t}{\Gamma(mN_r)\ln 2}\sum_{i=1}^{L}\Gamma(k_i) \times G_{4,2}^{1,4}\left[\frac{\gamma\Omega_i}{mLN_tD_i^\upsilon}\middle|\begin{matrix}1-k_i, 1-mN_r, 1, 1\\ 1, 0\end{matrix}\right] \quad (7)$$

where $G[\cdot]$ is the Meijer's G-function [17, eq. (9.301)].

Proof: We start by writing (6) through [10, eq. (64)]

$$C_{\text{up}} = N_t\sum_{i=1}^{L}\mathcal{E}\left[\log_2\left(1 + \frac{\gamma}{LN_t}\frac{\xi_i\psi_i}{D_i^\upsilon}\right)\right] \quad (8)$$

where $\psi_i, i = 1, \ldots, L$ is the sum of N_r i.i.d. gamma RVs and as such $\psi_i \sim \text{Gamma}(mNr, 1/m)$, or

$$p(\psi_i) = \frac{\psi_i^{mN_r-1}}{\Gamma(mN_r)}m^{mNr}\exp\left(-m\psi_i\right), \quad \psi_i \geq 0. \quad (9)$$

[1]In the following, it is assumed that $LN_t \leq N_r$ (i.e., $s = LN_t, t = N_r$). All results though are very easily extensible to the case $LN_t > N_r$.

We now express the expectation in (8) in integral form

$$C_{\text{up}} = \frac{N_t}{\ln 2}\sum_{i=1}^{L}\int_0^\infty\int_0^\infty \ln\left(1 + \frac{\gamma\xi_i\psi}{LN_tD_i^\upsilon}\right)p(\psi)p(\xi_i)d\psi d\xi_i = \frac{N_t}{\ln 2}\sum_{i=1}^{L}\int_0^\infty\int_0^\infty G_{2,2}^{1,2}\left[\frac{\gamma\xi_i\psi}{LN_tD_i^\upsilon}\middle|\begin{matrix}1,1\\1,0\end{matrix}\right]p(\psi)p(\xi_i)d\psi d\xi_i \quad (10)$$

where (10) follows by expressing the logarithmic function via [18, eq. (8.4.6.5)]. Substituting (2) and (9) into (10), applying [17, eq. (7.813.1)] we can obtain (7) after some algebra. ■

Comparing (7) with [10, eq. (22)], we clearly observe that the proposed bound admits an analytical and more tractable expression and thus can efficiently characterize the capacity of composite Nakagami-m/gamma fading MIMO channels.

Theorem 2: For $\{k_i, m, k_i - mN_r\} \notin \mathbb{Z}$, the ergodic capacity in (5) is upper bounded by (11) shown at the bottom of the page, where ${}_pF_q(\cdot)$ denotes the generalized hypergeometric function while $\psi(x)$ is the Euler's digamma function [17, eq. (8.360.1)].

Proof: A detailed proof is given in Appendix I. ■

Theorem 3: In the high-SNR regime C_{up} in (7) becomes

$$C_{\text{up}}^\infty = LN_t\log_2\left(\frac{\gamma}{LN_t}\right) + \frac{LN_t}{\ln 2}\left(\psi(mN_r) - \ln(m)\right) + N_t\sum_{i=1}^{L}\left(\frac{\psi(k_i)}{\ln 2} + \log_2(\Omega_i) - \upsilon\log_2(D_i)\right). \quad (12)$$

Proof: The result follows by taking γ large in (8), then using the integral identity [17, eq. (4.352.1)]

$$\int_0^\infty x^{\nu-1}e^{-\mu x}\ln x dx = \frac{\Gamma(\nu)}{\mu^\nu}(\psi(\nu) - \ln\mu) \quad (13)$$

for $\text{Re}(\mu, \nu > 0)$, and simplifying the resulting expression. ■

The above theorem reveals that at high SNRs the effects of small and large-scale fading are decoupled, which is consistent with [10, Corollary 5]. More important, it turns out that taking the SNR large in (11) leads to exactly the same high-SNR approximation of (12). This implies that (11) offers an inherent differentiation of the low and high-SNR terms.

IV. Capacity Analysis of K MIMO Channels

When the small-scale fading is described via the Rayleigh distribution (i.e., $m = \Omega = 1$), the fading model is referred to as the K-distribution [15], [16], which has recently attracted considerable research interest thanks to its ability to effectively approximate the fading fluctuations in various radar and RF communication systems [11], [12].

$$C_{\text{up}} = \frac{N_t}{\ln 2}\sum_{i=1}^{L}\left[\frac{\left(\frac{LN_tmD_i^\upsilon}{\gamma\Omega_i}\right)^{k_i}\Gamma(1-k_i)\Gamma(mN_r-k_i)\,{}_1F_2\left(k_i; k_i+1, k_i+1-mN_r; -\frac{LN_tmD_i^\upsilon}{\gamma\Omega_i}\right)}{k_i\Gamma(mN_r)} + \frac{\left(\frac{LN_tmD_i^\upsilon}{\gamma\Omega_i}\right)^{mN_r}\Gamma(k_i-mN_r)\Gamma(1-mN_r)\,{}_1F_2\left(mN_r; 1-k_i, k_i+1+mN_r; -\frac{LN_tmD_i^\upsilon}{\gamma\Omega_i}\right)}{mN_r\Gamma(k_i)} + \frac{LN_tmD_i^\upsilon}{\gamma\Omega_i(k_i-1)(mN_r-1)}\,{}_2F_3\left(1,1; 2, 2-k_i, 2-mN_r; -\frac{LN_tmD_i^\upsilon}{\gamma\Omega_i}\right) + \psi(k_i) + \psi(mN_r) - \ln\left(\frac{LN_tmD_i^\upsilon}{\gamma\Omega_i}\right)\right]. \quad (11)$$

A. Low-SNR Analysis

The low-SNR performance of K MIMO channels can be investigated by taking a first-order expansion of (4) around $\gamma = 0^+$. Recent theoretic studies have demonstrated though that this approach can not adequately reflect the impact of the channel and can, in fact, lead to misleading results in the low-SNR (or wideband) regime [19], [20]. Thus, it is more meaningful to explore the low-SNR capacity in terms of the normalized transmit energy per information bit E_b/N_0 rather than per-symbol SNR. This capacity representation reads as

$$C_{\rm erg}\left(\frac{E_b}{N_0}\right) \approx \mathcal{S}_0 \log_2\left(\frac{\frac{E_b}{N_0}}{\frac{E_b}{N_{0\,\min}}}\right) \tag{14}$$

where $E_b/N_{0\min}$ and $\mathcal{S}_0$ are the two key parameters determining the low-SNR behavior, corresponding to the "minimum normalized energy per information bit required to convey any positive rate reliably" and the wideband slope, respectively. Following [19], these two figures of merit are defined as

$$\frac{E_b}{N_{0\,\min}} = \frac{1}{\dot{C}_{\rm erg}(0)}, \quad \mathcal{S}_0 = -2\ln 2 \frac{\left(\dot{C}_{\rm erg}(0)\right)^2}{\ddot{C}_{\rm erg}(0)} \tag{15}$$

where $\dot{C}_{\rm erg}(\cdot)$ and $\ddot{C}_{\rm erg}(\cdot)$ denote the first and second-order derivatives of the ergodic capacity (5) over the SNR γ, respectively.

Corollary 1: For K fading MIMO channels, the minimum energy per information bit and the wideband slope are

$$\frac{E_b}{N_{0\,\min}} = \frac{L\ln 2}{N_r}\left(\sum_{i=1}^{L}\frac{k_i\Omega_i}{D_i^{\upsilon}}\right)^{-1}$$

$$\mathcal{S}_0 = \frac{2N_tN_r\left(\sum_{i=1}^{L}\frac{k_i\Omega_i}{D_i^{\upsilon}}\right)^2}{N_t\left(\sum_{i=1}^{L}\frac{k_i\Omega_i}{D_i^{\upsilon}}\right)^2 + N_r\sum_{i=1}^{L}k_i(k_i+1)\left(\frac{\Omega_i}{D_i^{\upsilon}}\right)^2}. \tag{16}$$

Proof: We first recall that

$$\frac{d}{dx}\ln\left(\det\left(\mathbf{I}+x\mathbf{A}\right)\right)\big|_{x=0} = \mathrm{tr}(\mathbf{A}). \tag{17}$$

As such, we need to evaluate

$$\mathcal{E}\left[\mathrm{tr}\left(\mathbf{Z}^{\dagger}\mathbf{Z}\right)\right] = N_t\sum_{i=1}^{L}\int_0^{\infty}\int_0^{\infty}\frac{\xi_i\psi}{D_i^{\upsilon}}p(\psi)p(\xi_i)d\psi d\xi_i. \tag{18}$$

Substituting (2) and (9) into (18) and applying [17, eq. (3.381.4)]

$$\int_0^{\infty}x^{\nu}\exp(-\mu x) = \mu^{-(\nu+1)}\Gamma(\nu+1),\ \mathrm{Re}(\mu,\nu)>0 \tag{19}$$

we can obtain (16) after basic simplifications. For $\mathcal{S}_0$, we invoke a classical result from random matrix theory on correlated Rayleigh MIMO channels [20, eq. (19)]. Substituting $\mathbf{\Theta}_{\rm R} = \mathbf{I}_{N_r}$ and $\mathbf{\Theta}_{\rm T} = \mathbf{\Xi}$ in [20, eq. (19)], we can work out the final expression by averaging over $\mathbf{\Xi}$, again with the aid of (19). ∎

Note that (16) is independent of N_t, which agrees with [19], [20], while a higher N_r improves the low-SNR capacity by reducing $E_b/N_{0\min}$. Under i.i.d. Rayleigh fading, we simply have

$$\frac{E_b}{N_{0\,\min}} = \frac{\ln 2}{N_r}, \quad \mathcal{S}_0 = \frac{2N_tN_r}{N_t+N_r} \tag{20}$$

which respectively coincide with [19, eq. (206)], [20, eq. (17)], and [20, eq. (19)] (i.e., for $\mathbf{\Theta}_{\rm R} = \mathbf{I}_{N_r}$ and $\mathbf{\Theta}_{\rm T} = \mathbf{I}_{LN_t}$).

B. High-SNR Analysis

We now focus on the first- and second-order MI statistics in the high-SNR regime. More specifically, the following theorem yields the ergodic capacity in the high-SNR regime:

Theorem 4: For K fading MIMO channels, the ergodic capacity at high SNRs tends to

$$C_{\rm erg}^{\infty} = s\log_2\left(\frac{\gamma}{LN_t}\right) + \frac{1}{\ln 2}\sum_{i=0}^{s-1}\psi(t-i) + N_t\sum_{i=1}^{L}\left(\frac{\psi(k_i)}{\ln 2} + \log_2(\Omega_i) - \upsilon\log_2(D_i)\right). \tag{21}$$

Proof: A detailed proof is given in Appendix II. ∎

Clearly, both k_i and Ω_i have a beneficial impact on the high-SNR capacity whereas a higher Tx-Rx distance effectively reduces it, due to the increased path-loss attenuation.

Apart from the ergodic capacity, a critical figure of merit in the performance evaluation of MIMO systems is the variance of the MI which can give better insights into the outage capacity characterization. For this reason, the following result on the high-SNR MI variance is rather intuitive:

Theorem 5: For K fading MIMO channels, the variance of the MI at high SNRs tends to

$$\mathrm{Var}[\mathcal{I}^{\infty}] = \frac{1}{(\ln 2)^2}\sum_{i=0}^{s-1}\psi'(t-i) + \frac{N_t}{(\ln 2)^2}\sum_{i=1}^{L}\zeta(2,k_i) \tag{22}$$

where $\psi'(x) = d\psi(x)/dx$ is the polygamma function [21, eq. (6.4.1)], while $\zeta(z,q)$, $\mathrm{Re}(z) > 0$, $q \neq 0,-1,-2,\ldots$ is the Harwitz zeta function [17, eq. (9.521.1)].

Proof: A detailed proof is relegated to Appendix III. ∎

This theorem demonstrates that the MI variance converges to a deterministic constant for large SNR. Interestingly, the mean and variance of MI are not related which implies that macro-diversity has no impact on the ergodic capacity.

To get a better insight into the high-SNR capacity performance, we now introduce the affine capacity expansion [22]

$$C_{\rm erg}(\gamma, L, N_t, N_r) = \mathcal{S}_{\infty}\left(\log_2\gamma - \mathcal{L}_{\infty}\right) + o(1) \tag{23}$$

where $\mathcal{S}_{\infty}$ is the *high-SNR slope* in bits/s/Hz per 3-dB units

$$\mathcal{S}_{\infty} = \lim_{\gamma\longrightarrow\infty}\frac{C_{\rm erg}(\gamma,L,N_t,N_r)}{\log_2(\gamma)} \tag{24}$$

while $\mathcal{L}_{\infty}$ is the *high-SNR power offset*, in 3-dB units,

$$\mathcal{L}_{\infty} = \lim_{\gamma\longrightarrow\infty}\left(\log_2(\gamma) - \frac{C_{\rm erg}(\gamma,L,N_t,N_r)}{\mathcal{S}_{\infty}}\right). \tag{25}$$

Corollary 2: For K fading MIMO channels, the high-SNR slope and power offset are

$$\mathcal{S}_{\infty} = s$$

$$\mathcal{L}_{\infty} = \log_2(s) - \frac{1}{LN_t\ln 2}\sum_{i=0}^{s-1}\psi(t-i) \tag{26}$$

$$- \frac{1}{L}\sum_{i=1}^{L}\left(\frac{\psi(k_i)}{\ln 2} + \log_2(\Omega_i) - \upsilon\log_2(D_i)\right). \tag{27}$$

Proof: The proof follows trivially by combining (5), (21) and Appendix II with the definitions (24) and (25). ∎

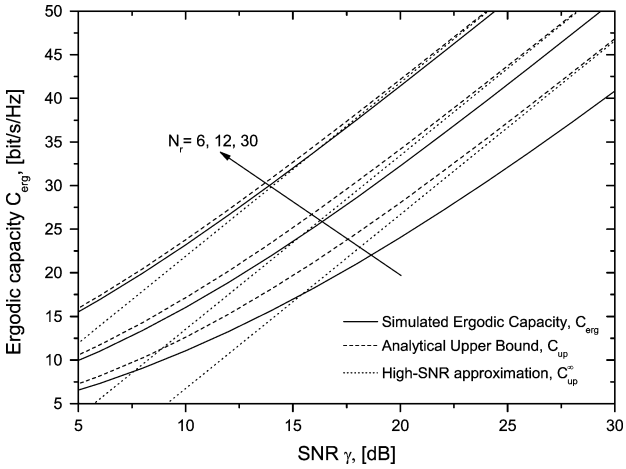

Fig. 1. Simulated ergodic capacity, analytical upper bound and high-SNR bound approximation against the SNR ($N_t = 2$, $L = 3$, $\upsilon = 4$, $m = 1/2$, $k_i = 1, \Omega_i = 2, D_1 = 1000\,\mathrm{m}$, $D_2 = 1500\,\mathrm{m}$, $D_3 = 2000\,\mathrm{m}$).

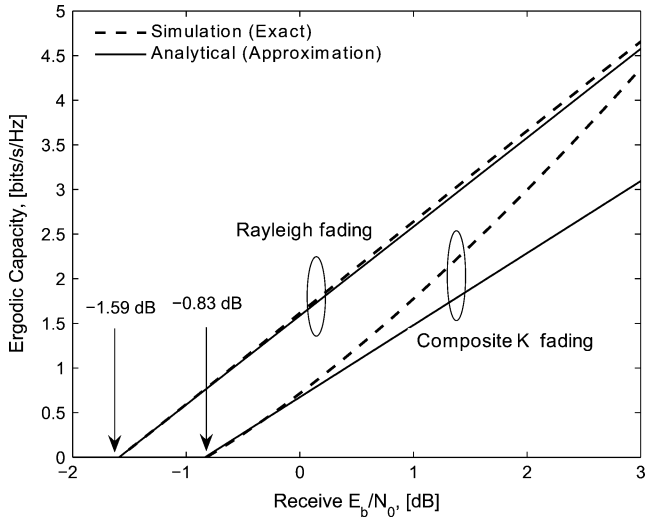

Fig. 2. Low-SNR simulated and analytical ergodic capacity against the received energy per bit ($N_r = 6$, $N_t = 2$, $L = 3$, $m = 1$).

The relationship (26) verifies the well-known asymptotic (in terms of SNR) linear capacity scaling with the minimum number of antennas [1]–[3]. In addition, (27) indicates that for a fixed number of transmit antennas, using more antennas at the receiver leaves the high-SNR slope unaffected but increases the high-SNR capacity by reducing the power offset.

C. Lower Bound

We finally introduce the following tight and rather simple lower bound on the ergodic capacity of K MIMO channels:

Theorem 6: For K fading MIMO channels, the ergodic capacity (5) is lower bounded by

$$C_{\mathrm{lb}} = s\log_2\left(1+\frac{\gamma}{LN_t}\exp\left(\frac{1}{s}\left(\sum_{i=0}^{s-1}\psi\left(t-i\right)\right.\right.\right.$$
$$\left.\left.\left.+N_t\sum_{i=1}^{L}\left(\psi(k_i)+\ln\left(\Omega_i\right)-\upsilon\ln(D_i)\right)\right)\right)\right). \quad (28)$$

Proof: The proof relies on the application of Minkowski's inequality to (5), as was originally proposed in [3, Theorem 1] and thereafter in [4, eq. (41)]. Omitting explicit details, we can directly lower bound (5) according to

$$C_{\mathrm{erg}} \le s\log_2\left(1+\frac{\gamma}{LN_t}\exp\left(\frac{1}{s}\mathcal{E}\left[\ln\left(\det\left(\mathbf{Z}^{\dagger}\mathbf{Z}\right)\right)\right]\right)\right)$$

and then we follow the methodology of Appendix II. ∎

Comparing (21) with (28), we can see that the lower bound converges to the exact high-SNR ergodic capacity. Note that similar observations were also made in [3], [4].

V. Numerical Results

In this section, the theoretical analysis presented in Sections III and IV is validated through a set of Monte-Carlo simulations. To this end, we first generate 10,000 random realizations of the large and small-scale fading matrices $\boldsymbol{\Xi}$ and $\mathbf{H}$ according to (2) and (3), respectively and thereafter obtain the simulated ergodic capacity via (5). In Fig. 1, the simulated ergodic capacity is compared against the analytical upper bound in (7) and the high-SNR approximation in (12). For the sake of simplicity, we have set $k_i = 1, \Omega_i = 2, \forall i = 1, \ldots, L$. A high N_r makes the bound tighter while the high-SNR approximation becomes exact even at moderate SNR values. In the low-SNR regime, the bound converges asymptotically to the empirical value of ergodic capacity [3]–[5].

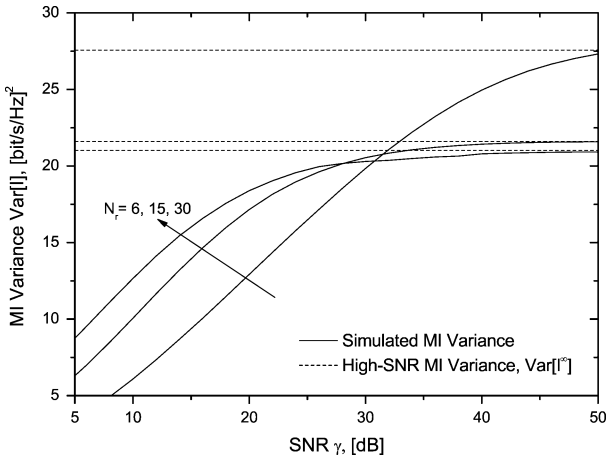

Fig. 3. Simulated and high-SNR approximation of the variance of the MI against the SNR ($N_t = 2$, $L = 3$, $\upsilon = 4$, $m = 1$).

In Fig. 2, the analytical and simulated low-SNR capacity are depicted against the received energy per bit $E_b^r/N_0 = N_r E_b/N_0$, based on (14). The capacity of a 6×2 i.i.d. Rayleigh MIMO channel is also overlaid where (20) has been used. The presence of large-scale fading reduces both the low-SNR channel throughput and also the wideband slope. It turns out that the linear approximations are accurate over a moderate range of E_b^r/N_0 values, especially for the Rayleigh case.

In Fig. 3, the variance of the MI is plotted with the high-SNR approximation being generated via (22). The graph reveals that increasing N_r helps overcome the effects of fading (i.e., enhanced receive spatial diversity) and, consequently, the dynamic range of MI is reduced. The convergence speed of the simulated curves to the asymptotic values gets also higher with N_r. In all cases, we see that the results converge quickly to the asymptotic values even for moderate values of the SNR.

VI. Conclusion

The capacity characterization of composite Nakagami-m MIMO channels is a particularly interesting research topic which however can not be addressed via Wishart matrix theory. Based on some recent results on majorization theory, we derived a novel analytical upper bound for the ergodic capacity of MIMO channels experiencing Nakagami/gamma fading. The proposed bound is more tractable than a previously derived bound for Nakagami/lognormal channels. In the second part, a detailed capacity characterization of K fading MIMO channels was performed and affine capacity expansions were proposed in the low and high-SNR regimes. For high SNRs, tractable closed-form approximations for the first- and second-order capacity moments were proposed. Finally, a simple lower capacity bound was given which becomes exact at high SNRs.

Appendix I
Proof of Theorem 2

The proof starts by noting that the general upper bound in (7) does not, in principle, admit a hypergeometric series expansion due to the arguments of the involved Meijer's G-function being integer [17, Sec. 9.31]. Thus, we have to adopt a different line of reasoning by rewriting (6) according to

$$C_{\text{up}} = \frac{N_t m^{mN_r}}{\Gamma(mN_r)\ln 2}\sum_{i=1}^{L}\frac{1}{\Gamma(k_i)\,\Omega_i^{k_i}} \times \int_0^\infty\int_0^\infty \ln\left(1+\frac{\gamma\xi_i\psi}{LN_tD_i^v}\right) \times \psi^{mN_r-1}\xi_i^{k_i-1}e^{(-\xi_i/\Omega_i - m\psi)}d\psi d\xi_i.$$

In order to solve the above double integral, we now provide a generic expression for integrals of the form

$$\mathcal{I}_1(a,b,p,z,w) = \int_0^\infty \mathcal{I}_2(a,p,zx)\,x^{b-1}\exp\left(-\frac{x}{w}\right)dx \quad (29)$$

where

$$\mathcal{I}_2(a,p,c) = \int_0^\infty \ln(1+cy)\,y^{a-1}\exp(-py)\,dy. \quad (30)$$

Using [18, eq. (2.6.23.4)], (30) admits a closed-form solution when $a \notin \mathbb{Z}$, as below

$$\mathcal{I}_2(a,p,c) = \left(\frac{1}{c}\right)^a \frac{\pi}{a\sin(a\pi)}{}_1F_1\left(a;a+1;\frac{p}{c}\right) -\Gamma(a)\,p^{-a}\left\{\ln\left(\frac{p}{c}\right)-\psi(a)-\frac{{}_2F_2\left(1,1;2,2-a;\frac{p}{c}\right)}{b(a-1)}\right\}.$$

By defining

$$\mathcal{J}_1 = \frac{\pi z^{-a}}{a\sin(a\pi)}\int_0^\infty x^{b-a-1}{}_1F_1\left(a;a+1;\frac{p}{zx}\right)e^{(-x/w)}dx$$

$$\mathcal{J}_2 = \Gamma(a)\,p^{-a}\int_0^\infty\left(\ln\left(\frac{p}{zx}\right)-\psi(a)\right)x^{b-1}e^{(-x/w)}dx$$

$$\mathcal{J}_3 = \frac{\Gamma(a)\,p^{-a}}{b(a-1)}\int_0^\infty x^{b-1}{}_2F_2\left(1,1;2,2-a;\frac{p}{zx}\right)e^{(-x/w)}dx$$

we rewrite (29) according to

$$\mathcal{I}_1(a,b,p,z,w) = \mathcal{J}_1 - \mathcal{J}_2 + \mathcal{J}_3. \quad (31)$$

We can solve $\mathcal{J}_1$ by expressing the hypergeometric function ${}_1F_1(\cdot)$ via a Meijer's G-function, using [23, eq. (07.20.26.0005.01)] and [17, eq. (9.31.2)], as

$${}_1F_1\left(a;a+1;\frac{p}{zx}\right) = \frac{\pi\Gamma(1+a)}{\Gamma(a)}G_{3,2}^{1,1}\left[\frac{zx}{p}\middle|\begin{matrix}1,1+a,\frac{1}{2}\\ a,\frac{1}{2}\end{matrix}\right]$$

and after introducing [17, eq. (7.813.1)], we can obtain

$$\mathcal{J}_1 = \frac{\pi^2}{\sin(a\pi)\,z^a}\left(\frac{1}{w}\right)^{a-b}G_{4,2}^{1,4}\left[\frac{wz}{p}\middle|\begin{matrix}1-b+a,1,1+a,\frac{1}{2}\\ a,\frac{1}{2}\end{matrix}\right]. \quad (32)$$

The last formula can be further simplified by combining [17, eq. (9.304)] and [23, eq. (07.26.03.0002.01)] with (32)

$$\mathcal{J}_1 = \frac{\pi^2}{\sin(a\pi)\,z^a}\left(\frac{1}{w}\right)^{a-b} \times\left(\frac{\Gamma(a-b)\left(\frac{wz}{p}\right)^{-b+a}{}_1F_2\left(b;1+b-a,1+b;-\frac{p}{wz}\right)}{b\Gamma\left(\frac{1}{2}+b-a\right)\Gamma\left(\frac{1}{2}-b+a\right)}\right. +\left.\frac{\Gamma(b-a)}{a\pi}{}_1F_2\left(a;1+a,1+a-b;-\frac{p}{wz}\right)\right) \quad (33)$$

when $\{a,b,b-a\}\notin\mathbb{Z}$. Likewise, $\mathcal{J}_2$ can be rewritten as

$$\mathcal{J}_2 = \Gamma(a)\,p^{-a}\int_0^\infty(\ln(p)-\ln(zx)-\psi(a))\,x^{b-1}e^{(-x/w)}dx$$

which, according to [18, eq. (2.6.21.2)], simplifies to

$$\mathcal{J}_2 = \Gamma(a)\,p^{-a}\Gamma(b)\,w^b\left(\ln\left(\frac{p}{wz}\right)-\psi(a)-\psi(b)\right). \quad (34)$$

For $\mathcal{J}_3$, we expand the integrand ${}_2F_2(\cdot)$ using [23, eq. (07.25.26.0004.01)] and [17, eq. (9.31.2)], or

$${}_2F_2\left(1,1;2,2-a;\frac{p}{zx}\right) = \pi\Gamma(2-a)\,G_{4,3}^{2,1}\left[\frac{zx}{p}\middle|\begin{matrix}1,2,2-a,\frac{1}{2}\\ 1,1,\frac{1}{2}\end{matrix}\right]$$

and after introducing [17, eq. (7.813.1)], we can obtain

$$\mathcal{J}_3 = \frac{\pi\Gamma(a-1)\,\Gamma(2-a)\,p^{-a+1}w^{b-1}}{z} \times G_{5,3}^{2,2}\left[\frac{wz}{p}\middle|\begin{matrix}2-b,1,2,2-a,\frac{1}{2}\\ 1,1,\frac{1}{2}\end{matrix}\right]. \quad (35)$$

When $\{a,b,b-a\}\notin\mathbb{Z}$, the last expression can be expanded via [17, eq. (9.304)] and [23, eq. (07.31.03.0002.01)], to get

$$\mathcal{J}_3 = \frac{\Gamma(a-1)\,\Gamma(2-a)\,p^{-a+1}w^{b-1}\pi}{z} \times\left(\frac{\Gamma(b)\,\Gamma(1-b)\left(\frac{wz}{p}\right)^{1-b}{}_1F_2\left(b;1+b,1+b-a;-\frac{p}{wz}\right)}{b\Gamma(1-a+b)\,\Gamma\left(b-\frac{1}{2}\right)\Gamma\left(\frac{3}{2}-b\right)}\right. +\left.\frac{\Gamma(b-1)}{\pi\Gamma(2-a)}{}_2F_3\left(1,1;2,2-a,2-b;-\frac{p}{wz}\right)\right). \quad (36)$$

We now combine (33), (34), and (36) with (31). The result in (11) is obtained after substituting the appropriate values for all parameters, i.e., $a=k_i$, $b=mN_r$, $p=1/\Omega_i$, $z=\gamma/LN_tD_i^v$, $\omega=1/m$ and thereafter using the Euler's reflection formula $\pi/\sin(\pi x) = \Gamma(x)\Gamma(1-x)$ [21, eq. (6.1.17)] along with $\Gamma(x+1)=x\Gamma(x)$ [21, eq. (6.1.15)] to simplify.

Appendix II
Proof of Theorem 4

The proof starts by rearranging (5) as

$$C_{\text{erg}} = \mathcal{E}\left[\log_2\left(\det\left(\mathbf{I}_{LN_t}+\frac{\gamma}{LN_t}\boldsymbol{\Xi}\mathbf{H}^\dagger\mathbf{H}\right)\right)\right] \quad (37)$$

where we have used the following determinant property: $\det(\mathbf{I}_n + \mathbf{A}_{n\times m}\mathbf{B}_{m\times n}) = \det(\mathbf{I}_m + \mathbf{B}_{m\times n}\mathbf{A}_{n\times m})$. Then, as $\gamma \to \infty$, the ergodic capacity in (5) simplifies to

$$C_{\text{erg}}^{\infty} = s\log_2\left(\frac{\gamma}{LN_t}\right) + \frac{1}{\ln 2}\mathcal{E}\left[\ln\left(\det\left(\mathbf{\Xi}\right)\right)\right] + \frac{1}{\ln 2}\mathcal{E}\left[\ln\left(\det\left(\mathbf{H}^{\dagger}\mathbf{H}\right)\right)\right]. \quad (38)$$

Since $\mathbf{H}$ is Rayleigh distributed, the term $\mathbf{H}^{\dagger}\mathbf{H}$ follows a central (zero-mean) Wishart distribution [1]–[5]. Using [2, eq. (A.8.1)], we can directly express the last term in (38) as

$$\mathcal{E}\left[\ln\left(\det\left(\mathbf{H}^{\dagger}\mathbf{H}\right)\right)\right] = \sum_{i=0}^{s-1}\psi\left(t-i\right). \quad (39)$$

Since $\mathbf{\Xi}$ is diagonal, the second term in (38) is evaluated as

$$\mathcal{E}\left[\ln\left(\det\left(\mathbf{\Xi}\right)\right)\right] = \mathcal{E}\left[\ln\left(\prod_{i=1}^{LN_t}\xi_i D_i^{-v}\right)\right] \quad (40)$$

$$= -N_t\sum_{i=1}^{L}\ln\left(D_i\right)^{v} + N_t\sum_{i=1}^{L}\mathcal{E}\left[\ln\left(\xi_i\right)\right] \quad (41)$$

$$\overset{(13)}{=} -N_t v\sum_{i=1}^{L}\ln\left(D_i\right) + N_t\sum_{i=1}^{L}\left(\psi(k_i) + \ln(\Omega_i)\right). \quad (42)$$

Combining (38), (39) and (42) we can easily obtain (21).

Appendix III
Proof of Theorem 5

The proof follows a similar line of reasoning as in Theorem 4. In general, the variance of the MI is given by

$$\text{Var}[\mathcal{I}] = \mathcal{E}[\mathcal{I}^2] - \mathcal{E}^2[\mathcal{I}]. \quad (43)$$

Omitting explicit details, we express the MI variance in the high-SNR regime according to

$$\text{Var}[\mathcal{I}^{\infty}] = \text{Var}\left[\log_2\left(\det\left(\frac{\gamma}{LN_t}\mathbf{\Xi}\mathbf{H}^{\dagger}\mathbf{H}\right)\right)\right]$$

$$= \frac{1}{(\ln 2)^2}\left(\text{Var}\left[\ln\left(\det\left(\mathbf{\Xi}\right)\right)\right] + \text{Var}\left[\ln\left(\det\left(\mathbf{H}^{\dagger}\mathbf{H}\right)\right)\right]\right). \quad (44)$$

The second term in (44) was given in [2, eq. (A.8.2)]

$$\text{Var}\left[\ln\left(\det\left(\mathbf{H}^{\dagger}\mathbf{H}\right)\right)\right] = \sum_{i=0}^{s-1}\psi'\left(t-i\right) \quad (45)$$

while the first term of (44), after taking into account that the gamma variates are i.i.d., evaluates as

$$\text{Var}\left[\ln\left(\det\left(\mathbf{\Xi}\right)\right)\right] = N_t\sum_{i=1}^{L}\text{Var}\left[\ln\left(\xi_i\right)\right]$$

$$\overset{(43)}{=} N_t\sum_{i=1}^{L}\left(\int_o^{\infty}\ln^2\left(\xi_i\right)p(\xi_i)d\xi_i - \left(\psi(k_i)+\ln(\Omega_i)\right)^2\right). \quad (46)$$

The proof concludes after substituting (2) into (46), using the integral identity [17, eq. (4.358.2)]

$$\int_0^{\infty} x^{\nu-1}e^{-\mu x}\ln^2 x dx = \frac{\Gamma(\nu)}{\mu^{\nu}}\left(\left(\psi(\nu)-\ln\mu\right)^2 + \zeta(2,\nu)\right)$$

for $\text{Re}(\mu,\nu > 0)$ and simplifying.

References

[1] I. E. Telatar, "Capacity of multi-antenna Gaussian channels," *Europ. Trans. Telecommun.*, vol. 10, no. 6, pp. 585–595, Nov./Dec. 1999.

[2] A. Grant, "Rayleigh fading multi-antenna channels," *EURASIP J. Appl. Signal Process.*, vol. 2002, no. 3, pp. 316–329, Mar. 2002.

[3] Ö. Oyman, R. Nabar, H. Bölcskei, and A. Paulraj, "Characterizing the statistical properties of mutual information in MIMO channels," *IEEE Trans. Signal Process.*, vol. 51, no. 11, pp. 2782–2795, Nov. 2003.

[4] M. R. McKay and I. B. Collings, "General capacity bounds for spatially correlated rician MIMO channels," *IEEE Trans. Inf. Theory*, vol. 51, no. 9, pp. 3121–3145, Sep. 2005.

[5] M. Matthaiou, Y. Kopsinis, D. I. Laurenson, and A. M. Sayeed, "Upper bound for the ergodic capacity of dual MIMO Ricean systems: Simplified derivation and asymptotic tightness," *IEEE Trans. Commun.*, vol. 57, pp. 3589–3596, Dec. 2009.

[6] H. Suzuki, "A statistical model for urban radio propagation," *IEEE Trans. Commun.*, vol. 25, pp. 673–679, Jul. 1997.

[7] M. Matthaiou, D. I. Laurenson, and J. S. Thompson, "A MIMO channel model based on the Nakagami-faded spatial eigenmodes," *IEEE Trans. Antennas Propag.*, vol. 56, no. 5, pp. 1494–1497, May 2008.

[8] M. Nakagami, "The m-distribution-A general formula of intensity distribution of rapid fading," in *Statistical Methods in Radio Wave Propagation*, W. C. Hoffman, Ed. Oxford, U.K.: Pergamon, 1960, pp. 3–36.

[9] G. Fraidenraich, O. Leveque, and J. M. Cioffi, "On the MIMO channel capacity for the Nakagami-m channel," *IEEE Trans. Inf. Theory*, vol. 54, no. 8, pp. 3752–3757, Aug. 2008.

[10] C. Zhong, K.-K. Wong, and S. Jin, "Capacity bounds for MIMO Nakagami-m fading channels," *IEEE Trans. Signal Process.*, vol. 57, no. 9, pp. 3613–3623, Sep. 2009.

[11] P. M. Shankar, "Error rates in generalized shadowed fading channels," *Wireless Personal Commun.*, vol. 28, no. 3, pp. 233–238, Feb. 2004.

[12] P. S. Bithas, N. C. Sagias, P. T. Mathiopoulos, G. K. Karagiannidis, and A. A. Rontogiannis, "On the performance analysis of digital communications over generalized-K fading channels," *IEEE Commun. Lett.*, vol. 10, pp. 353–355, May 2006.

[13] I. M. Kostić, "Analytical approach to performance analysis for channel subject to shadowing and fading," *Proc. Inst. Electr. Eng.—Commun.*, vol. 152, no. 6, pp. 821–827, Dec. 2005.

[14] A. Laourine, M. -S. Alouini, S. Affes, and A. Stéphenne, "On the capacity of generalized-K fading channels," *IEEE Trans. Wireless Commun.*, vol. 7, no. 7, pp. 2441–2445, Jul. 2008.

[15] A. Abdi and M. Kaveh, "K distribution: An appropriate substitute for Rayleigh-lognormal distribution in fading-shadowing wireless channels," *IEE Electron. Lett.*, vol. 34, no. 9, pp. 851–852, Apr. 1998.

[16] A. Abdi and M. Kaveh, "Comparison of DPSK and MSK bit error rates for K and Rayleigh-lognormal fading distributions," *IEEE Commun. Lett.*, vol. 4, pp. 122–124, Apr. 2000.

[17] I. S. Gradshteyn and I. M. Ryzhik, *Table of Integrals, Series, and Products*, 7th ed. San Diego, CA: Academic, 2007.

[18] A. P. Prudnikov, Y. A. Brychkov, and O. I. Marichev, *Integrals and Series*. New York: Gordon & Breach, 1990, vol. 3, More Special Functions.

[19] S. Verdú, "Spectral efficiency in the wideband regime," *IEEE Trans. Inf. Theory*, vol. 48, no. 6, pp. 1319–1343, Jun. 2001.

[20] A. Lozano, A. M. Tulino, and S. Verdú, "Multiple-antenna capacity in the low-power regime," *IEEE Trans. Inf. Theory*, vol. 49, no. 10, pp. 2527–2544, Oct. 2003.

[21] M. Abramowitz and I. A. Stegun, *Handbook of Mathematical Functions with Formulas, Graphs, and Mathematical Tables*, 9th ed. New York: Dover, 1970.

[22] S. Shamai (Shitz) and S. Verdú, "The impact of frequency-flat fading on the spectral efficiency of CDMA," *IEEE Trans. Inf. Theory*, vol. 47, no. 4, pp. 1302–1327, May 2001.

[23] Wolfram, The Wolfram Functions Site [Online]. Available: http://functions.wolfram.com